Dynamical weight functions for a planar crack

A. A. Al-Falou,[1] R. C. Ball,[1] and H. Larralde[2]
[1]University of Warwick, Coventry CV4 7AL, United Kingdom
[2]Centro de Ciencias Fisicas, UNAM, Avenida Universida, Col. Chamilpa, Cuernavaca, Morelos, Mexico
(Received 3 August 1999)

The stress intensity factors are evaluated for a moving planar crack for loadings which vary arbitrarily in time and three dimensions of space. We exploit the adjoint elasticity equation obeyed by the corresponding weight functions, and a new and more universal Wiener-Hopf factorization of the Rayleigh function, this being the central difficulty in such calculations. For the mode II weight function we give further asymptotic results crucial to a subsequent calculation of crack stability with respect to out-of-plane perturbations.

PACS number(s): 46.50.+a, 62.20.Mk, 05.45.−a, 83.50.−v

I. INTRODUCTION

The first part of our work revolves around the calculation and properties of the dynamical weight functions. Weight functions are Green functions which by definition return the stress intensity factors at a point Z along the crack tip and time T for a given volume force $\underline{f}$ and boundary traction $\underline{g}$ [1], e.g., for mode I,

$$K_{\mathrm{I}}(T,Z)=\int dt\int_{\Omega} d^3x\, \underline{W}_{\mathrm{I}}(T,Z,t,\underline{x})\cdot \underline{f}(t,\underline{x}) + \int dt \int_{\partial\Omega} dS\, \underline{W}_{\mathrm{I}}(T,Z,t,\underline{x}(S))\cdot \underline{g}(t,\underline{x}(S)), \tag{1}$$

where Ω and $\partial\Omega$ are the domain and the boundary of the cracking material, and analogously for modes II and III.

We will take our crack to propagate in the x direction in the x,z plane, with the crack edge along the z direction and the normal to the fracture plane in the y direction. Then qualitatively, in terms of stress components diverging ahead of the crack, K_{I} corresponds to normal stresses (notably σ_{yy}), K_{II} to shearing in the x direction (σ_{xy}) and K_{III} to shearing in the z direction (σ_{yz}).

Type I crack propagation, driven by K_{I}, is the most natural case to consider as its stress field has the full symmetry of the planar crack geometry. The pure type II stress field is antisymmetric with respect to the y direction (out of plane), and hence K_{II} plays a central role in the discussion of the stability of type I cracks with respect to out-of-plane perturbation. For this reason the full type II weight function is a crucial input to the crack stability calculations of our following paper [2], and we discuss it here in greatest detail. We include an evaluation of type I and III weight functions in the present paper for completeness. In our following paper we consider the self-consistent evolution of a perturbed crack through the surface $y=h(x,z)$, to first order in $h(x,z)$; for stability, elementary self-consistent solutions must decrease as x increases.

The most general definition of a weight function $\underline{W}$ is that $\underline{W}(x,y,z,t)\cdot \underline{p}$ returns some particular stress intensity factor at some particular time and position along the edge of the crack, in response to a point impulse $\underline{p}$ applied to the material at x,y,z,t. The direct approach to computing $\underline{W}$ would be to to compute the full displacement field resulting from the impulse, and then to extract the stress intensity factors as the coefficients of its leading behavior around the crack tip. This could all be done via the full elastic Green function of the material (with its time dependent boundary), which directly gives the displacements resulting from arbitrary forces; extracting the stress intensity factors then amounts to taking a projection from the Green function.

It follows that the weight functions inherit from the Green function the property that they obey the equations of elasticity (strictly their adjoint, but they are self-adjoint)

$$\frac{\partial^2}{\partial t^2}\underline{W} - \boldsymbol{\nabla}\cdot \mathbf{C}:\boldsymbol{\nabla}\underline{W}=0 \quad \text{in} \quad \Omega$$

and

$$\underline{n}\cdot \mathbf{C}:\boldsymbol{\nabla}\underline{W}=0 \quad \text{on} \quad \partial\Omega, \tag{2}$$

where $\mathbf{C}$ is the elasticity tensor and $\underline{n}$ the boundary surface normal. Discussion of inhomogeneous terms at the crack tip, inherited from the Green function equation, is obviated by requiring the weight functions to match the near crack asymptotic form of simple known cases.

The approach outlined above is not dependent on any particular crack shape or motion (provided it is specified), nor material inhomogeneity or isotropy. Historically it was first communicated in the context of quasi-static cracks by Bueckner [3] in 1970 and by Rice [4] in 1972 as a corollary of Betti's theorem [1]. It was actually used by Bueckner [5] to calculate the quasistatic (i.e., negligible velocity) weight functions and by Freund [1] to calculate the two-dimensional weight functions for time-dependent loadings. The general space and time dependent case for a moving crack was discussed explicitly by Willis and Mouvchan [6,7], but in a representation where the equations of elasticity appear non-self-adjoint. Strictly speaking it is the adjoint of the elasticity equations which appears in Eq. (2); see also Ref. [8]. As a result the simple general form of Bueckner's results remain under appreciated.

For a planar crack the conditions across the fracture plane present a natural problem for the application of Wiener-Hopf techniques, with boundary conditions applying over the fractured half of the plane and continuity conditions applying across the unfractured half. We refer the reader to Freund's [1] book for a good introduction to the Wiener-Hopf technique in this context.

Willis and Mouvchan already published a calculation of the dynamical surface weight functions (corresponding to loadings on the crack surface only) along these lines, leading to results in terms of one coordinate dependent quadrature. Our work differs in using a new and more explicit factorization of the Rayleigh function, which is universal up to dependence on Poisson's ratio. This leads to significantly more explicit results for all three weight functions, which in the case of mode II are crucial for crack stability calculations in our following paper. We also go beyond Willis and Mouvchan in considering loadings applied to points inside the material, rather than just on the fracture surface. Our main results are given explicitly in *y*, but Fourier-Laplace transformed with respect to *x*, *z*, and *t*. In the type II case we elaborate further detail at the crack surface, and also in terms of *x* and *y* near the crack tip.

In the context of weight functions we find it useful to distinguish between the quasistatic case, that is zero crack velocity, and the dynamical weight functions for general velocity. In either case, we distinguish further between (1) the two-dimensional weight function (a function of x,y), corresponding to loadings uniformly distributed over the third dimension *z* if any, or $k_z=0$ in Fourier terms; (2) the surface weight function (a function of x,z), corresponding to loadings on the crack faces in three dimensions; and (3) the general three-dimensional weight function for loadings arbitrarily located in *x*, *y*, and *z*.

II. MODE II WEIGHT FUNCTION FOR A MOVING CRACK AND TIME-DEPENDENT LOADINGS

Our calculation of the weight functions is based on the fact that the dynamical weight function for a moving planar crack is determined by the homogeneous equations of elasticity and the leading order divergence near the crack tip. We hereby avoid loading contributions in the Wiener Hopf equations. The discussion of the weight function properties in the quasistatic case [8] translates similarly to the dynamical crack. Hence we are looking for a solution of the homogeneous equations of elasticity which generates zero loadings on the crack face and which diverges as $1/\sqrt{r}$ near the crack tip. The remaining undetermined constant can be found by comparison with the known two-dimensional weight function. Here we present details for the mode II case. The adaptation to modes I and III is straightforward, and we collect results for all three cases in Sec. III below.

Our strategy to obtain the dynamical weight function in Fourier space consists of four steps. First, we express the weight function in terms of the Lamé potentials for which the equations of elasticity translate into two sets of wave equations and the corresponding boundary conditions. Second, we establish the correspondence between semi-infinite support in real space and (upwards or downwards) analyticity in Fourier space. Third, we use the boundary conditions to arrive at two (decoupled) sets of Wiener-Hopf equations for the Lamé potentials. In each Wiener-Hopf equation we have terms with mixed upwards and downwards analyticity. The key to unraveling the Wiener-Hopf equations into a downward analytic function on one side of the equation and an upward analytic function on the other is to factorize the Rayleigh function. We can then use the identity theorem to continue each side analytically in the whole complex plane. In the fourth and last step, we apply Liouville's theorem to arrive at the final expressions for the Fourier transformed Lamé potentials. We then substitute the Lamé potentials to obtain the components of the mode II weight function.

In our first step we express the weight function $\underline{W}_{\rm II}$ and the generated stress field $\underline{\underline{\sigma}}=\mathbf{C}:\boldsymbol{\nabla}\underline{W}_{\rm II}$ in terms of the Lamé potentials Φ and $\underline{\Psi}$ (see also Freund's book [1]),

$$W_{{\rm II},x}=\frac{\partial\Phi}{\partial x}+\frac{\partial\Psi_3}{\partial y}-\frac{\partial\Psi_2}{\partial z},$$

$$W_{{\rm II},y}=\frac{\partial\Phi}{\partial y}+\frac{\partial\Psi_1}{\partial z}-\frac{\partial\Psi_3}{\partial x},\quad W_{{\rm II},z}=\frac{\partial\Phi}{\partial z}+\frac{\partial\Psi_2}{\partial x}-\frac{\partial\Psi_1}{\partial y}, \tag{3}$$

where the vector field $\underline{\Psi}$ must satisfy the additional gauge condition $\boldsymbol{\nabla}\cdot\underline{\Psi}=0$:

$$\frac{\sigma_{xy}}{\mu}=2\frac{\partial^2\Phi}{\partial x\partial y}+\frac{\partial^2\Psi_3}{\partial y^2}-\frac{\partial^2\Psi_2}{\partial y\partial z}-\frac{\partial^2\Psi_3}{\partial x^2}+\frac{\partial^2\Psi_1}{\partial x\partial z}, \tag{4}$$

$$\frac{\sigma_{yy}}{\mu}=\frac{c_D^2}{c_S^2}\nabla^2\Phi-2\frac{\partial^2\Phi}{\partial z^2}-2\frac{\partial^2\Phi}{\partial x^2}+2\frac{\partial^2\Psi_1}{\partial y\partial z}-2\frac{\partial^2\Psi_3}{\partial x\partial y}, \tag{5}$$

$$\frac{\sigma_{yz}}{\mu}=2\frac{\partial^2\Phi}{\partial y\partial z}+\frac{\partial^2\Psi_1}{\partial z^2}-\frac{\partial^2\Psi_3}{\partial x\partial z}-\frac{\partial^2\Psi_1}{\partial y^2}+\frac{\partial^2\Psi_2}{\partial x\partial y}. \tag{6}$$

The remaining stress components are not listed here as they do not enter the boundary conditions (they can be found in Freund's book [1]). As all the derivatives above are at constant time *t* we are at liberty to replace *x* by the variable $X=x-vt$ in the comoving frame.

In what follows we work in the comoving frame of reference and all fields are Fourier transformed with respect to their *z* coordinate. As from the symmetry of mode II we know that the first and second components of the mode II weight function are symmetric in *z*, whereas the third component is antisymmetric. Applying this symmetry to the *z* dependence, for a single Fourier component we can write

$$\begin{aligned}\Phi(X,y,z,t)&=\Phi(X,y,t)\cos(k_z z),\\ \Psi_1(X,y,z,t)&=\Psi_1(X,y,t)\sin(k_z z),\\ \Psi_2(X,y,z,t)&=\Psi_2(X,y,t)\sin(k_z z),\\ \Psi_3(X,y,z,t)&=\Psi_3(X,y,t)\cos(k_z z).\end{aligned} \tag{7}$$

In the comoving frame, the potentials obey the wave equations

$$\left[\frac{1}{c_D^2}\left(\frac{\partial}{\partial t}-v\frac{\partial}{\partial X}\right)^2-\left(\frac{\partial^2}{\partial X^2}+\frac{\partial^2}{\partial y^2}-k_z^2\right)\right]\Phi=0, \tag{8}$$

$$\left[\frac{1}{c_S^2}\left(\frac{\partial}{\partial t}-v\frac{\partial}{\partial X}\right)^2-\left(\frac{\partial^2}{\partial X^2}+\frac{\partial^2}{\partial y^2}-k_z^2\right)\right]\underline{\Psi}=0, \qquad (9)$$

where c_D and c_S are the dilation and shear wave speeds and the vector field $\underline{\Psi}$ has been taken to satisfy the gauge condition $\nabla\cdot\underline{\Psi}=0$.

In our second step, we consider symmetries with respect to y and establish the analyticity properties of the weight function and the generated stress fields in Fourier space. The first and third components of $\underline{W}_{\mathrm{II}}$ are antisymmetric in y [in the sense $f(-y)=-f(y)$], whereas the second component is symmetric. On the upper crack surface and its continuation ahead of the crack ($y=0^+$) we have

$$W_{\mathrm{II},x}=\begin{cases}0, & X>0\\ W_x^-(X,t)\cos(k_z z), & X<0\end{cases}$$

and

$$W_{\mathrm{II},z}=\begin{cases}0, & X>0\\ W_z^-(X,t)\sin(k_z z), & X<0.\end{cases} \qquad (10)$$

The minus (or plus) sign in the upper index indicates that the function is nonzero for negative (or positive) X only. Clearly, it suffices to work in the upper half space ($y\geqslant 0$) since the corresponding fields in the lower half space can be obtained by symmetry. These symmetries with respect to y and the zero loadings on the crack face ($X\leqslant 0$) yield the following boundary conditions on the upper surface $y=0^+$:

$$\sigma_{xy}=\begin{cases}\sigma_{xy}^+(X,t)\cos(k_z z), & X>0\\ 0, & X<0,\end{cases} \qquad \sigma_{yy}=0,$$

$$\sigma_{yz}=\begin{cases}\sigma_{yz}^+(X,t)\sin(k_z z), & X>0\\ 0, & X<0.\end{cases} \qquad (11)$$

The plus index indicates that σ_{xy} is zero for $X\leqslant 0$ and $y=0$, for example. We now apply a (two-sided) Laplace transform in time and a Fourier transform in X to the fields Φ, $\underline{\Psi}$, $\underline{W}_{\mathrm{II}}$, and $\underline{\underline{\sigma}}$. Our convention for the two-side Laplace transform and the Fourier transform in X is given by

$$\Phi(X,y,t)=\int_{c-i\infty}^{c+i\infty}ds\, e^{st}\frac{1}{2\pi}\int_{-\infty}^{\infty}dk_x e^{ik_xX}\hat{\Phi}(s,y,k_x) \qquad (12)$$

and

$$\hat{\Phi}(s,y,k_x)=\int_{-\infty}^{0}dt\, e^{-st}\int_{-\infty}^{\infty}dX\, e^{-ik_xX}\Phi(X,y,t). \qquad (13)$$

Note that we have used the causality of the weight functions in the last equation, i.e., only past loadings contribute to the stress intensity factor. Hence the upper limit of the integral is 0 instead of ∞.

By comparison with the quasistatic weight function [8] we anticipate that the (with respect to z Fourier transformed) weight function, and hence the stress field $\underline{\underline{\sigma}}$, are exponentially bounded in X, say by $e^{-\alpha|X|}$. This means that the Fourier transform of W^- is analytic in the upper complex plane for $\mathrm{Im}(k_x)>-\alpha$, and the Fourier transform of σ^+ is analytic in the lower complex plane as $\mathrm{Im}(k_x)<\alpha$. This motivates the notation $\hat{W}^u(k_x)$ for the Fourier transform of W^- and $\hat{\sigma}^d(k_x)$ for the Fourier transform of σ^+, respectively.

The solutions of the transformed wave equations (8) and (9), which are bounded in the upper half plane $y\geqslant 0$, are given by

$$\hat{\Phi}(k_x,y,s)=\hat{\Phi}(k_x,s)e^{-\gamma_D y},\quad \hat{\underline{\Psi}}(k_x,y,s)=\hat{\underline{\Psi}}(k_x,s)e^{-\gamma_S y}, \qquad (14)$$

where

$$\gamma_D^2=k_x^2+k_z^2+\frac{1}{c_D^2}(s-vik_x)^2,$$

$$\gamma_S^2=k_x^2+k_z^2+\frac{1}{c_S^2}(s-vik_x)^2. \qquad (15)$$

We also use the definition

$$\alpha_n=\sqrt{1-\frac{v^2}{c_n^2}},\quad n=S,D,R. \qquad (16)$$

In the third step, we turn our attention to the boundary conditions which yield the final Wiener-Hopf equations. First we set the solutions in Eqs. (14) into the transformed equations (4)–(6). Then we rewrite the boundary equations in terms of the newly defined potentials

$$\chi_1=k_z\frac{\hat{\sigma}_{xy}}{\mu}+ik_x\frac{\hat{\sigma}_{yz}}{\mu},\quad \chi_2=ik_x\frac{\hat{\sigma}_{xy}}{\mu}+k_z\frac{\hat{\sigma}_{yz}}{\mu},$$

$$\Lambda_1=k_z\hat{W}_{\mathrm{II},x}+ik_x\hat{W}_{\mathrm{II},z},\quad \Lambda_2=ik_x\hat{W}_{\mathrm{II},x}+k_z\hat{W}_{\mathrm{II},z}. \qquad (17)$$

The reason for introducing the new potentials is to decouple the final Wiener-Hopf equations later in the calculation. The boundary ($y=0^+$) values of χ and Λ are given in terms of those of Φ and $\underline{\Psi}$:

$$\chi_1^d=\gamma_S^2(k_z\hat{\Psi}_3-ik_x\hat{\Psi}_1)+(k_z^2+k_x^2)\gamma_S\hat{\Psi}_2, \qquad (18)$$

$$\chi_2^d=2(k_z^2+k_x^2)\gamma_D\hat{\Phi}+(\gamma_S^2+k_z^2+k_x^2)(ik_x\hat{\Psi}_3-k_z\hat{\Psi}_1), \qquad (19)$$

$$\Lambda_1^u=-(k_z^2+k_x^2)\hat{\Psi}_2-\gamma_S(k_z\hat{\Psi}_3-ik_x\hat{\Psi}_1), \qquad (20)$$

$$\Lambda_2^u=-(k_z^2+k_x^2)\hat{\Phi}-\gamma_S(ik_x\hat{\Psi}_3-k_z\hat{\Psi}_1), \qquad (21)$$

and the boundary conditions are implied by the upwards (u) or downwards (d) analyticity of χ_1, χ_2, Λ_1, and Λ_2, respectively. Additionally, we have $\hat{\sigma}_{yy}=0$ and the gauge condition $0=\nabla\cdot\underline{\Psi}$, i.e.,

$$0=(\gamma_S^2+k_z^2+k_x^2)\hat{\Phi}+2\gamma_S(ik_x\hat{\Psi}_3-k_z\hat{\Psi}_1), \qquad (22)$$

$$0=-ik_x\hat{\Psi}_1+\gamma_S\hat{\Psi}_2+k_z\hat{\Psi}_3. \qquad (23)$$

Elimination of $\hat{\Phi}$ and $\hat{\underline{\Psi}}$ from Eqs. (18)–(23) yields

$$\chi_1^d = -\gamma_S \Lambda_1^u, \tag{24}$$

$$\chi_2^d = -\frac{r(k_x)}{\gamma_S(\gamma_S^2 - k_z^2 - k_x^2)} \Lambda_2^u, \tag{25}$$

where

$$r(k_x) = (k_z^2 + k_x^2 + \gamma_S^2)^2 - 4\gamma_S \gamma_D (k_x^2 + k_z^2). \tag{26}$$

Equations (24) and (25) are crucial because they encode the weight function as a pair of Wiener-Hopf problems (see below). Given solutions for Λ_1 and Λ_2, we can then substitute back to obtain the Fourier transformed components of the weight function.

The spirit of the Wiener-Hopf calculation rests on the splitting of the factors γ_S in Eq. (24) and $r(k_x)/\gamma_S(\gamma_S^2 - k_z^2 - k_x^2)$ in Eq. (25) into a product of a downwards and an upwards analytic function. The Wiener-Hopf factorization of Eq. (24) is

$$\gamma_S = \gamma_S^u \gamma_S^d = \sqrt{\alpha_S i(i\omega^u(c_S) - k_x)} \sqrt{\alpha_S i(k_x - i\omega^d(c_S))}, \tag{27}$$

where

$$\omega^u(c_n) = \omega^u\left(c_n, \frac{s}{v|k_z|}\right) = \frac{|k_z|}{\alpha_n^2}\left[\frac{s}{v|k_z|}\frac{v^2}{c_n^2} - \sqrt{\alpha_n^2 + \left(\frac{s}{v|k_z|}\right)^2 \frac{v^2}{c_n^2}}\right],$$

$$\omega^d(c_n) = \omega^d\left(c_n, \frac{s}{v|k_z|}\right) = \frac{|k_z|}{\alpha_n^2}\left[\frac{s}{v|k_z|}\frac{v^2}{c_n^2} + \sqrt{\alpha_n^2 + \left(\frac{s}{v|k_z|}\right)^2 \frac{v^2}{c_n^2}}\right], \tag{28}$$

where $n = S,D,R$, and $i\omega^u(c_n)$ and $i\omega^d(c_n)$ are the branch points of γ_n^u and γ_n^d, respectively. Note that $i\omega^u(c_n)$ lies in the lower half-plane but corresponds to the branch analytic in the upper half-plane, and vice versa, for $i\omega^d(c_n)$. Note that we chose the branch cut of the complex square root to be on the negative real axis. With this definition the first square root in Eq. (27) is upward analytic, whereas the second is downward analytic.

A key difficulty in our evaluation consists of factorizing the second Wiener-Hopf equation in Eq. (25), that is, the factorization of the Rayleigh function $r(k_x)$ into downward and upward sectionally analytic functions. Following Freund [1] the factorization takes the form

$$r(k_x) = -D\left(ik_x - \frac{s}{v}\right)^2 (ik_x + \omega^u(c_R)) \times (ik_x + \omega^d(c_R)) S^u(k_x) S^d(k_x), \tag{29}$$

where ω^u and ω^d are defined in Eq. (27); this renders explicit all the zeros of $r(k_x)$ and the constant $D = 4\alpha_S\alpha_D - (1 + \alpha_S^2)^2$ is chosen such that $S^u(k_x)S^d(k_x) \to 1$ as $|k_x| \to \infty$. The factor $S^u(k_x)$ is upward analytic and the factor $S^d(k_x)$ is downward analytic. Obtaining explicit expressions or approximations of $S^u(k_x)$ and $S^d(k_x)$ is the major computational challenge, which we discuss in Sec. IV below.

We can now decompose the Wiener-Hopf equations in Eqs. (24) and (25) into upward and downward analytic functions with a joint strip of analyticity:

$$\frac{1}{\gamma_S^d}\chi_1^d = -\gamma_S^u \Lambda_1^u, \tag{30}$$

$$\frac{\gamma_S^d}{(ik_x + \omega^d(c_R))S^d}\chi_2^d = \frac{D}{1-\alpha_S^2}\frac{(ik_x + \omega^u(c_R))S^u}{\gamma_S^u}\Lambda_2^u. \tag{31}$$

According to the identity theorem in complex analysis, each side in Eq. (30) is analytic in the whole complex plane.

We have now arrived at the fourth and last step of the Wiener-Hopf calculation, that is, the identification of Λ_1 and Λ_2 on the grounds of Liouville's theorem and boundedness arguments. As in the quasistatic case [8], we know by dimensional arguments that the most divergent term of the three-dimensional weight function in real space diverges like $1/\sqrt{r}$, and it is identical to the two-dimensional weight function. As the two-dimensional weight function has a zero z component, we conclude that $W_{\mathrm{II},z} \sim \sqrt{r}$ as $r = \sqrt{x^2+y^2} \to 0$. The other components in real space diverge like $W_{\mathrm{II},x} \sim 1/\sqrt{r}$, $W_{\mathrm{II},y} \sim 1/\sqrt{r}$, and hence, $\sigma_{xy} \sim 1/r\sqrt{r}$ and $\sigma_{yz} \sim 1/\sqrt{r}$ as $r \to 0$. Therefore, $\Lambda_1 \sim k_z/\sqrt{k_x}$, $\Lambda_2 \sim \sqrt{k_x}$, $\chi_1 \sim k_z\sqrt{k_x}$, and $\chi_2 \sim k_x\sqrt{k_x}$ as $|k_x| \to \infty$. Applying Liouville's theorem to the analytic functions in Eq. (30), we have

$$\frac{1}{\gamma_S^d}\chi_1^d = c_0 k_z = -\gamma_S^u \Lambda_1^u, \tag{32}$$

$$\frac{\gamma_S^d}{(ik_x + \omega^d(c_R))S^d}\chi_2^d = c_0 c_1 |k_z| + c_0 c_2 i k_x = \frac{D}{1-\alpha_S^2}\frac{(ik_x + \omega^u(c_R))S^u}{\gamma_S^u}\Lambda_2^u, \tag{33}$$

where we have defined the Liouville constants such that c_0, c_1, and c_2 are dimensionless quantities. The constants c_1 and c_2 are determined in the following, whereas we are left with an overall constant c_0 as we work with the homogeneous equations of elasticity. Combining Eqs. (32), (32), and (17) we obtain $\hat{W}_{\mathrm{II},x}$ and $\hat{W}_{\mathrm{II},z}$ on $y = 0^+$:

$$\frac{\hat{W}_{\mathrm{II},x}(k_x, 0^+, k_z)}{c_0} = \frac{1}{k_x^2 + k_z^2} \times \left[-\frac{k_z^2}{\gamma_S^u} - \frac{1-\alpha_S^2}{D}\frac{ik_x(c_1|k_z| + c_2 i k_x)}{(ik_x + \omega^u(c_R))}\frac{\gamma_S^u}{S^u}\right] \tag{34}$$

$$\frac{\hat{W}_{\mathrm{II},z}(k_x,0^+,k_z)}{c_0}=\frac{1}{k_x^2+k_z^2}\times\left[\frac{ik_xk_z}{\gamma_S^u}+\frac{1-\alpha_S^2}{D}\frac{k_z(c_1|k_z|+c_2ik_x)}{(ik_x+\omega^u(c_R))}\frac{\gamma_S^u}{S^u}\right]. \tag{35}$$

Likewise, for the generated stress fields $\hat{\sigma}_{xy}$ and $\hat{\sigma}_{yz}$ we have

$$\frac{\hat{\sigma}_{xy}}{c_0\mu}=\frac{1}{k_x^2+k_z^2}\left(k_z^2\gamma_S^d-ik_x\frac{(ik_x+\omega^d(c_R))S^d}{\gamma_S^d}\times(c_1|k_z|+c_2ik_x)\right), \tag{36}$$

$$\frac{\hat{\sigma}_{yz}}{c_0\mu}=\frac{1}{k_x^2+k_z^2}\left(-ik_xk_z\gamma_S^d+k_z\frac{(ik_x+\omega^d(c_R))S^d}{\gamma_S^d}\times(c_1|k_z|+c_2ik_x)\right). \tag{37}$$

At this point, we can determine the constants c_1 and c_2. We recall that $\hat{W}_{\mathrm{II},x}$ and $\hat{W}_{\mathrm{II},z}$ are upward analytic functions, but in Eqs. (34) and (35) both appear to have a pole in the upper half plane at $k_x=i|k_z|$. To remove the pole the term in square brackets must be zero at $k_x=i|k_z|$,

$$0=k_z^2D(ik_x+\omega^u(c_R))S^u(k_x)+(1-\alpha_S^2)(\gamma_S^u(k_x))^2ik_x(c_1|k_z|+c_2ik_x), \tag{38}$$

at $k_x=i|k_z|$. Similarly, we know that $\hat{\sigma}_{xy}$ and $\hat{\sigma}_{yz}$ are downward analytic functions, and hence, the numerators in Eqs. (36) and (37) must be zero at $k_x=-i|k_z|$,

$$0=k_z^2(\gamma_S^d(k_x))^2-ik_x(ik_x+\omega^d(c_R))(c_1|k_z|+c_2ik_x)S^d(k_x), \tag{39}$$

at $k_x=-i|k_z|$. Equations (38) and (39) determine the constants c_1 and c_2:

$$c_1=c_1\left(\frac{s}{v|k_z|}\right)=\frac{1}{2}\left[-\frac{D}{\alpha_S(1-\alpha_S^2)}\frac{(|k_z|-\omega^u(c_R))S^u(i|k_z|)}{(|k_z|-\omega^u(c_S))}+\frac{\alpha_S(|k_z|+\omega^d(c_S))}{(|k_z|+\omega^d(c_R))S^d(-i|k_z|)}\right], \tag{40}$$

$$c_2=c_2\left(\frac{s}{v|k_z|}\right)=\frac{1}{2}\left[\frac{D}{\alpha_S(1-\alpha_S^2)}\frac{(|k_z|-\omega^u(c_R))S^u(i|k_z|)}{(|k_z|-\omega^u(c_S))}+\frac{\alpha_S(|k_z|+\omega^d(c_S))}{(|k_z|+\omega^d(c_R))S^d(-i|k_z|)}\right]. \tag{41}$$

In the last step of our calculation we substitute back into the potentials $\hat{\Phi}$ and $\underline{\hat{\Psi}}$ in Eqs. (18)–(22). We then use Eq. (3) to obtain the final expressions for all components of the Fourier transformed mode II weight function:

$$\hat{W}_{\mathrm{II},x}(k_x,y,k_z)=\frac{2ik_x\Lambda_2}{\gamma_S^2-k_x^2-k_z^2}(e^{-\gamma_Dy}-e^{-\gamma_Sy})+\frac{k_z\Lambda_1-ik_x\Lambda_2}{k_x^2+k_z^2}e^{-\gamma_Sy}, \tag{42}$$

$$\hat{W}_{\mathrm{II},y}(k_x,y,k_z)=\frac{\Lambda_2}{\gamma_S(\gamma_S^2-k_x^2-k_z^2)}\times[(\gamma_S^2+k_x^2+k_z^2)e^{-\gamma_Sy}-2\gamma_D\gamma_Se^{-\gamma_Dy}], \tag{43}$$

$$\hat{W}_{\mathrm{II},z}(k_x,y,k_z)=\frac{2k_z\Lambda_2}{\gamma_S^2-k_x^2-k_z^2}(e^{-\gamma_Sy}-e^{-\gamma_Dy})+\frac{k_z\Lambda_2-ik_x\Lambda_1}{k_x^2+k_z^2}e^{-\gamma_Sy}, \tag{44}$$

where $y\geqslant 0$ and Λ_1 and Λ_2 are defined in Eq. (17). Explicitly, they are given in Eqs. (32) and (33). At $y=0^+$ we recover the earlier results for $\hat{W}_{\mathrm{II},x}$ and $\hat{W}_{\mathrm{II},z}$ in Eqs. (34) and (35).

Finally, we shall determine the unknown constant c_0. For this purpose it is sufficient to evaluate the 3D weight function at $y=0^+$ and $s=0$ in the 2D limit $k_z\to 0$. If we apply this procedure to $\hat{W}_{\mathrm{II},x}$ in Eq. (42) we obtain

$$\hat{W}_{\mathrm{II},x}(k_x)=-i\frac{1-\alpha_S^2}{D}\sqrt{\alpha_S}c_0c_2(0,\alpha_n)\frac{\sqrt{-ik_x}}{k_x}. \tag{45}$$

Comparison with the known Fourier transformed 2D weight function in Appendix C yields

$$c_0=-\frac{D}{\sqrt{2\alpha_S}(1-\alpha_S^2)}\frac{1}{c_2(0,\alpha_n)}. \tag{46}$$

III. EXPLICIT FOURIER-TRANSFORMED WEIGHT FUNCTIONS

The weight functions for modes I and III are obtained by the same Wiener-Hopf method as above. Note that the only difference between the modes consists of the symmetries in *z* and *y* and the asymptotic behavior near the crack tip. In the case of mode I, $W_{\mathrm{I},x}$ and $W_{\mathrm{I},y}$ are symmetric in *z*, and $W_{\mathrm{I},z}$ is antisymmetric in *z*. Furthermore, $W_{\mathrm{I},y}$ is antisymmetric in *y*. Note in the following that $y\geqslant 0$. We have also added a table of symbols and definitions in Appendix A. The Wiener-Hopf procedure for mode I is simpler than in the case of mode II, and leads to

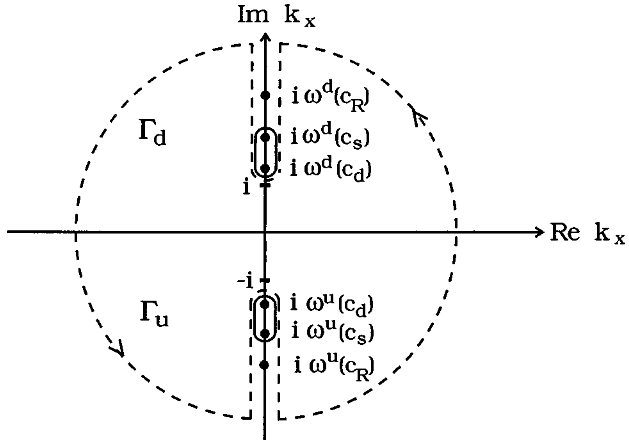

FIG. 1. The contour of integration and the position of the branch points for real s and $|s/v|k_z||\leqslant 1$, for the integration in Eq. (66). The two contributions Γ_u and Γ_d yield the separate factors of the Rayleigh function S^u and S^d, respectively.

$$\hat{W}_{\mathrm{I},x}(k_x,y,k_z,s)=\frac{W_{0,y}}{\gamma_S^2-k_x^2-k_z^2}\left[\frac{-ik_x}{\gamma_D}(\gamma_S^2+k_x^2+k_z^2)e^{-\gamma_D y}+2ik_x\gamma_S e^{-\gamma_S y}\right], \tag{47}$$

$$\hat{W}_{\mathrm{I},y}(k_x,y,k_z,s)=\frac{W_{0,y}}{\gamma_S^2-k_x^2-k_z^2}[(\gamma_S^2+k_x^2+k_z^2)e^{-\gamma_D y}-2(k_x^2+k_z^2)e^{-\gamma_S y}], \tag{48}$$

$$\hat{W}_{\mathrm{I},z}(k_x,y,k_z,s)=\frac{W_{0,y}}{\gamma_S^2-k_x^2-k_z^2}\times\left[\frac{k_z}{\gamma_D}(\gamma_S^2+k_x^2+k_z^2)e^{-\gamma_D y}-2k_z\gamma_S e^{-\gamma_S y}\right], \tag{49}$$

where

$$W_{0,y}=-\frac{1}{\sqrt{2\alpha_S}}\frac{\gamma_S^d}{(ik_x+\omega^u(c_R))S^u}. \tag{50}$$

The mode II weight function has been calculated in Sec. II. In summary we have

$$\hat{W}_{\mathrm{II},x}(k_x,y,k_z,s)=\frac{2ik_x\Lambda_2}{\gamma_S^2-k_x^2-k_z^2}(e^{-\gamma_D y}-e^{-\gamma_S y})+\frac{k_z\Lambda_1-ik_x\Lambda_2}{k_x^2+k_z^2}e^{-\gamma_S y}, \tag{51}$$

$$\hat{W}_{\mathrm{II},y}(k_x,y,k_z,s)=\frac{\Lambda_2}{\gamma_S(\gamma_S^2-k_x^2-k_z^2)}[(\gamma_S^2+k_x^2+k_z^2)e^{-\gamma_S y}-2\gamma_D\gamma_S e^{-\gamma_D y}], \tag{52}$$

$$\hat{W}_{\mathrm{II},z}(k_x,y,k_z,s)=\frac{2k_z\Lambda_2}{\gamma_S^2-k_x^2-k_z^2}(e^{-\gamma_S y}-e^{-\gamma_D y})+\frac{k_z\Lambda_2-ik_x\Lambda_1}{k_x^2+k_z^2}e^{-\gamma_S y}, \tag{53}$$

where

$$\Lambda_1=\frac{1}{\sqrt{2\alpha_S}c_2(0)}\frac{D}{1-\alpha_S^2}\frac{k_z}{\gamma_S^u}, \tag{54}$$

$$\Lambda_2=-\frac{1}{\sqrt{2\alpha_S}}\left(\frac{c_1\left(\frac{s}{v|k_z|}\right)}{c_2(0)}|k_z|+\frac{c_2\left(\frac{s}{v|k_z|}\right)}{c_2(0)}ik_x\right)\times\frac{\gamma_S^u}{(ik_x+\omega^u(c_R))S^u}, \tag{55}$$

$$c_1\left(\frac{s}{v|k_z|}\right)=\frac{1}{2}\left[-\frac{D}{\alpha_S(1-\alpha_S^2)}\frac{(|k_z|-\omega^u(c_R))S^u(i|k_z|)}{(|k_z|-\omega^u(c_S))}+\frac{\alpha_S(|k_z|+\omega^d(c_S))}{(|k_z|+\omega^d(c_R))S^d(-i|k_z|)}\right], \tag{56}$$

$$c_2\left(\frac{s}{v|k_z|}\right)=\frac{1}{2}\left[\frac{D}{\alpha_S(1-\alpha_S^2)}\frac{(|k_z|-\omega^u(c_R))S^u(i|k_z|)}{(|k_z|-\omega^u(c_S))}+\frac{\alpha_S(|k_z|+\omega^d(c_S))}{(|k_z|+\omega^d(c_R))S^d(-i|k_z|)}\right]. \tag{57}$$

The mode III weight functions have exactly the same symmetry in y as the mode II weight functions, but they have different z symmetry, that is, $W_{\mathrm{I},x}$ and $W_{\mathrm{I},y}$ are antisymmetric in z and $W_{\mathrm{I},z}$ is symmetric. Furthermore, the mode III has a reversed asymptotic behavior near the crack tip, i.e., $W_{\mathrm{I},x},W_{\mathrm{I},y}\sim\sqrt{r}$ and $W_{\mathrm{I},z}\sim 1/\sqrt{r}$. The same symmetry in y leads to solutions with similar structure to mode II:

$$\hat{W}_{\mathrm{III},x}(k_x,y,k_z,s)=\frac{2ik_x\Upsilon_2}{\gamma_S^2-k_x^2-k_z^2}(e^{-\gamma_D y}-e^{-\gamma_S y})-\frac{k_z\Upsilon_1+ik_x\Upsilon_2}{k_x^2+k_z^2}e^{-\gamma_S y}, \tag{58}$$

$$\hat{W}_{\mathrm{III},y}(k_x,y,k_z,s)=\frac{\Upsilon_2}{\gamma_S(\gamma_S^2-k_x^2-k_z^2)}[(\gamma_S^2+k_x^2+k_z^2)e^{-\gamma_S y}-2\gamma_D\gamma_S e^{-\gamma_D y}], \tag{59}$$

$$\hat{W}_{\mathrm{III},z}(k_x,y,k_z,s)=\frac{-2k_z\Upsilon_2}{\gamma_S^2-k_x^2-k_z^2}(e^{-\gamma_S y}-e^{-\gamma_D y})-\frac{k_z\Upsilon_2+ik_x\Upsilon_1}{k_x^2+k_z^2}e^{-\gamma_S y}, \tag{60}$$

where

$$\Upsilon_1 = -\frac{1}{\sqrt{2\alpha_S}\gamma_S^u}\left(\frac{d_1\left(\frac{s}{v|k_z|}\right)}{d_2(0)}|k_z| + \frac{d_2\left(\frac{s}{v|k_z|}\right)}{d_2(0)}ik_x\right), \tag{61}$$

$$\Upsilon_2 = \frac{1}{\sqrt{2\alpha_S}d_2(0)}\frac{1-\alpha_S^2}{D}\frac{\gamma_S^u}{(ik_x+\omega^u(c_R))S^u}, \tag{62}$$

$$d_1\left(\frac{s}{v|k_z|}\right) = -\frac{1}{2k_z}\left[-\frac{\alpha_S(1-\alpha_S^2)}{D}\frac{(|k_z|-\omega^u(c_S))}{(|k_z|-\omega^u(c_R))S^u(i|k_z|)} + \frac{(|k_z|+\omega^d(c_R))S^d(-i|k_z|)}{\alpha_S(|k_z|+\omega^d(c_S))}\right], \tag{63}$$

$$d_2\left(\frac{s}{v|k_z|}\right) = -\frac{1}{2k_z}\left[\frac{\alpha_S(1-\alpha_S^2)}{D}\frac{(|k_z|-\omega^u(c_S))}{(|k_z|-\omega^u(c_R))S^u(i|k_z|)} + \frac{(|k_z|+\omega^d(c_R))S^d(-i|k_z|)}{\alpha_S(|k_z|+\omega^d(c_S))}\right]. \tag{64}$$

IV. FACTORIZATION OF THE RAYLEIGH FUNCTION

We begin by discussing the conventional factorization, as discussed by Freund [1] and used by Willis and Mouvchan [6]. Then in the light of this we present our alternative which proves computationally much more explicit.

Factoring out the zeros of the Rayleigh function leads to

$$r(k_x) = -D\left(ik_x - \frac{s}{v}\right)^2(ik_x+\omega^u(c_R)) \times (ik_x+\omega^d(c_R))S^u(k_x)S^d(k_x), \tag{65}$$

where ω^u and ω^d are defined in Eq. (27). The function $S^u(k_x)S^d(k_x)$, which is defined by the last equation, has no zeros in the complex plane, it is bounded and the prefactor $D=4\alpha_S\alpha_D—(1+\alpha_S^2)^2$ is chosen such that $S^u(k_x)S^d(k_x)\to 1$ as $|k_x|\to\infty$. Hence the logarithm of $S^u(k_x)S^d(k_x)$ is defined in the whole complex plane and it approaches zero as $|k_x|\to\infty$. We follow Freund in the decomposition of $\ln(S^u(k_x)S^d(k_x))$ into two sectionally analytic functions $\ln S^u(k_x)$ and $\ln S^d(k_x)$. By means of Cauchy's integral, we obtain

$$\ln S^{u,d}(k_x) = \frac{1}{2\pi i}\int_{\Gamma_{u,d}} \ln\left(-\frac{(k_z^2+\tau^2+\gamma_S(\tau)^2)^2 - 4\gamma_S(\tau)\gamma_D(\tau)(\tau^2+k_z^2)}{D(i\tau-(s/v))^2(i\tau+\omega^u(c_R))(i\tau+\omega^d(c_R))}\right)\frac{d\tau}{\tau-k_x}, \tag{66}$$

which is equivalent to the form given by Willis and Mouvchan.

The contours of integration Γ_u and Γ_d are shown generically in Fig. 1, and can be collapsed down to simple integrals of the integrand discontinuity along the respective branch cuts. For real s the cuts lie on the imaginary axis and the integrals simplify down to

$$S^u(k_x) = \exp\left\{-\frac{1}{\pi}\int_{[\omega^u(c_S),\omega^u(c_D)]} \arctan\left(\frac{4(k_z^2-\tau^2)|\gamma_D(i\tau)\gamma_S(i\tau)|}{(\gamma_S(i\tau)^2+k_z^2-\tau^2)^2}\right)\frac{d\tau}{\tau+ik_x}\right\}, \tag{67}$$

$$S^d(k_x) = \exp\left\{\frac{1}{\pi}\int_{[\omega^d(c_D),\omega^d(c_S)]} \arctan\left(\frac{4(k_z^2-\tau^2)|\gamma_D(i\tau)\gamma_S(i\tau)|}{(\gamma_S(i\tau)^2+k_z^2-\tau^2)^2}\right)\frac{d\tau}{\tau+ik_x}\right\}. \tag{68}$$

This approach has the computational drawback of demanding a separate integration for each set of values of the variables k_x, k_z, and s (the last hidden implicitly in γ_S and γ_D), and for complex s keeping track of the branch cuts is computationally delicate. Compounded with Fourier integrals to transform back to real space, we found it too expensive to obtain real space weight functions.

Our alternative approach starts from the observation that

$$r(k_x) = \frac{(s-vik_x)^4}{c_S^4}R\left(\frac{-c_S^2(k_x^2+k_z^2)}{(s-vik_x)^2}\right), \tag{69}$$

where

$$R(u) = (1-2u)^2 + 4u\sqrt{1-u}\sqrt{\frac{c_S^2}{c_D^2}-u}. \tag{70}$$

The function $R(u)$ has one zero at $u_0=c_S^2/c_R^2$ and a branch cut along the real interval $[c_S^2/c_D^2,1]$. Our strategy is to express it in factors of the form

$$(u-u_j)^{\Delta\eta_j}, \quad c_S^2/c_D^2 \leq u_j < 1, \tag{71}$$

because such factors have a universal Wiener-Hopf factorization—see below.

Factoring out the zeros and its value at infinity, we have

$$R(u)=2\left(\frac{c_S^2}{c_D^2}-1\right)\left(u-\frac{c_S^2}{c_R^2}\right)f(u), \tag{72}$$

where $\ln f(u)\to 0$ as $|u|\to\infty$ and is analytic everywhere except the branch cut along the real interval $[c_S^2/c_D^2,1]$. We can now apply Cauchy's theorem to $\ln f(u)$ in the same spirit as Eqs. (66)–(68) to obtain

$$f(u)=\exp\left(\frac{1}{2\pi i}\int_{\text{branch cut}}\frac{\ln f(u')}{u'-u}du'\right) \tag{73}$$

$$=\exp\left(-\frac{1}{\pi}\int_{[c_S^2/c_D^2,1]}\arctan \times\frac{4u'\sqrt{1-u'}\sqrt{u'-c_S^2/c_D^2}}{(1-2u')^2}\frac{du'}{u'-u}\right). \tag{74}$$

Integrating by parts then leads to

$$f(u)=\exp\left(\int_0^{1/2}\ln\frac{u_1(\eta)-u}{u_2(\eta)-u}d\eta\right), \tag{75}$$

where $u_1(\eta)$ and $u_2(\eta)$ are the smaller and larger (real) roots of the equation

$$\eta(u)=\frac{1}{\pi}\arctan\frac{4u\sqrt{1-u}\sqrt{u-(c_S^2/c_D^2)}}{(1-2u)^2}, \tag{76}$$

as plotted in Fig. 2 (for Poisson's ratio $\nu=0.3$).

What makes this approach particularly fruitful is that we can decompose each term $u-u_1(\eta)$, and similarly $u-u_2(\eta)$, as follows:

$$u-u_1(\eta)=\frac{-c_S^2(k_x^2+k_z^2)}{(s-vik_x)^2}-u_1(\eta)=\frac{-c_S^2}{(s-vik_x)^2}\left(k_x^2+k_z^2+\frac{1}{(c_S/\sqrt{u_1(\eta)})^2}(s-vik_x)^2\right)$$

$$=\frac{c_S^2}{(s-vik_x)^2}\alpha\left(\frac{c_S}{\sqrt{u_1(\eta)}}\right)^2\left(k_x-i\omega^d\left(\frac{c_S}{\sqrt{u_1(\eta)}}\right)\right)\left(i\omega^u\left(\frac{c_S}{\sqrt{u_1(\eta)}}\right)-k_x\right), \tag{77}$$

where $\alpha(c)=\sqrt{1-(v^2/c^2)}$, and

$$\omega^u(c,s)=1/\alpha(c)^2(sv/c^2-\sqrt{\alpha(c)^2k_z^2+s^2/c^2}), \tag{78}$$

and the opposite sign of square root for $\omega^d(c,s)$ [also see Eq. (28)].

We now show that the roots $i\omega^u(c,s)$ and $i\omega^d(c,s)$ are trivially assigned correctly in Eq. (78), in the sense that $i\omega^u(c,s)$ remains in the lower complex plane and $i\omega^d(c,s)$ in the upper half plane for all complex s. We also rely on $v<c_S<c_S/\sqrt{u_1(\eta_j)}=c$. Here it is important that we take the standard convention that the square root function return non-negative real part, which leads to branch cuts outwards along the imaginary axis from $\pm i|k_z\alpha(c)c|$ for $\omega^u(c,s)$ and $\omega^d(c,s)$ in the complex plane.

For all real s the assignment of $\omega^u(c,s)$ and $\omega^d(c,s)$ is correct by inspection. Next we note that $\mathrm{Re}(\omega^{u,d})$ could only change sign on the imaginary axis of s, because for $\mathrm{Re}(\omega^{u,d})=0$, expression (77) would have a pure real root which is only possible for $\mathrm{Re}(s)=0$. Hence the assignments extend correctly from the real axis to each of the right and left half planes of s.

With Eqs. (72) and (73) the original function $r(k_x)$ in Eq. (69) can then be written

$$r(k_x)=2\left(\frac{1}{c_S^2}-\frac{1}{c_D^2}\right)(s-vik_x)^2\alpha_R^2[k_x-i\omega^u(c_R)][k_x-i\omega^d(c_R)]$$

$$\times\exp\left[\int_0^{1/2}\ln\frac{\alpha^2\left(\frac{c_S}{\sqrt{u_1(\eta)}}\right)\left(i\omega^u\left(\frac{c_S}{\sqrt{u_1(\eta)}}\right)-k_x\right)\left(k_x-i\omega^d\left(\frac{c_S}{\sqrt{u_1(\eta)}}\right)\right)}{\alpha^2\left(\frac{c_S}{\sqrt{u_2(\eta)}}\right)\left(i\omega^u\left(\frac{c_S}{\sqrt{u_2(\eta)}}\right)-k_x\right)\left(k_x-i\omega^d\left(\frac{c_S}{\sqrt{u_2(\eta)}}\right)\right)}d\eta\right]. \tag{79}$$

Using the above result that $i\omega^u(c,s)$ remains in the lower half-plane and $i\omega^d(c,s)$ in the upper half plane (for all complex s and $v \leqslant c_S$), respectively, and by comparison with Eq. (65), we can decompose $r(k_x)$ into a product of upwards and downwards analytic factors

$$S^u(k_x)=\exp\left[\int_0^{1/2}\ln\frac{i\omega^u\left(\frac{c_S}{\sqrt{u_1(\eta)}}\right)-k_x}{i\omega^u\left(\frac{c_S}{\sqrt{u_2(\eta)}}\right)-k_x}d\eta\right], \quad (80)$$

$$S^d(k_x)=\exp\left[\int_0^{1/2}\ln\frac{i\omega^d\left(\frac{c_S}{\sqrt{u_1(\eta)}}\right)-k_x}{i\omega^d\left(\frac{c_S}{\sqrt{u_2(\eta)}}\right)-k_x}d\eta\right], \quad (81)$$

where $\eta(u)$ is given Eq. (76) and $\omega^u(c)$, $\omega^d(c)$ were previously defined in Eq. (78). In the last equations we have also used the fact that $S^u(k_x),S^d(k_x)\rightarrow 1$ as $k_x\rightarrow\infty$.

Simple numerical quadrature schemes applied to the integrals in Eqs. (80) and (81) yield the desired factorization of the form

$$S^u(k_x)=\prod_{j=1}^{N}\left(\frac{k_x-i\omega^u\left(\frac{c_S}{\sqrt{u_1(\eta_j)}}\right)}{k_x-i\omega^u\left(\frac{c_S}{\sqrt{u_2(\eta_j)}}\right)}\right)^{\Delta\eta_j},$$

$$S^d(k_x)=\prod_{j=1}^{N}\left(\frac{k_x-i\omega^d\left(\frac{c_S}{\sqrt{u_1(\eta_j)}}\right)}{k_x-i\omega^d\left(\frac{c_S}{\sqrt{u_2(\eta_j)}}\right)}\right)^{\Delta\eta_j}. \quad (82)$$

We found Simpson's rule highly effective; using ten points for the case $\nu=0.3$ we obtain the exponents $\Delta\eta_j$ and the zeros $u_1(\eta_j)$ and $u_2(\eta_j)$ from

$$f(u)=\prod_{j=1}^{N}\left(\frac{u_1(\eta_j)-u}{u_2(\eta_j)-u}\right)^{\Delta\eta_j}=\left(\frac{u-0.499624}{u-0.500319}\right)^{1/60}\left(\frac{u-0.379559}{u-0.697455}\right)^{1/15}\left(\frac{u-0.348595}{u-0.789035}\right)^{1/30},$$
$$\left(\frac{u-0.329914}{u-0.854025}\right)^{1/15}\left(\frac{u-0.31682}{u-0.901582}\right)^{1/30}\left(\frac{u-0.306973}{u-0.936423}\right)^{1/15}\left(\frac{u-0.299344}{u-0.961645}\right)^{1/30}, \quad (83)$$
$$\left(\frac{u-0.293476}{u-0.979393}\right)^{1/15}\left(\frac{u-0.289219}{u-0.991136}\right)^{1/30}\left(\frac{u-0.286602}{u-0.997827}\right)^{1/15}\left(\frac{u-0.285714}{u-1}\right)^{1/60}.$$

It is important to note that this numerical quadrature in order to obtain $\Delta\eta_j$, $u_1(\eta_j)$, and $u_2(\eta_j)$, needs to be done once, and most importantly, independently of k_x, k_z, and s, for a given choice of c_S^2/c_D^2 (which is a function of Poisson's ratio only). We have also tested the factors $S^u(k_x)$ and $S^d(k_x)$ in Eq. (82) against their more conventional form in Eqs. (67) and (68) for real s. We have found that the relative numerical discrepancy is less than 0.0002 for all k_x along the real axis.

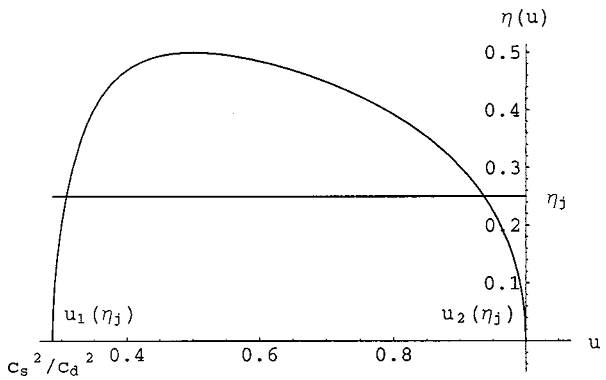

FIG. 2. The function $\eta(u)$ whose inverses $u_1(\eta)$ and $u_2(\eta)$ are used in Eq. (75), plotted for Poisson's ratio is $\nu=0.3$. $u_1(\eta)$ are to the left, $u_2(\eta)$ to the right.

V. NEAR CRACK TIP EXPANSION OF THE DYNAMICAL MODE II WEIGHT FUNCTION

At this point we anticipate the general structure of the stability analysis without elaborating on the details which shall be given in a future paper. As mentioned in Sec. I, the progress of a small perturbation $h(x,z)$ of the crack surface is determined by the criterion $K_{\rm II}[h(x,z)]=0$. The total mode II stress intensity factor $K_{\rm II}$ is decomposed as a sum of loading contributions from near the crack tip and loading contributions from the crack surface. Hence we require a

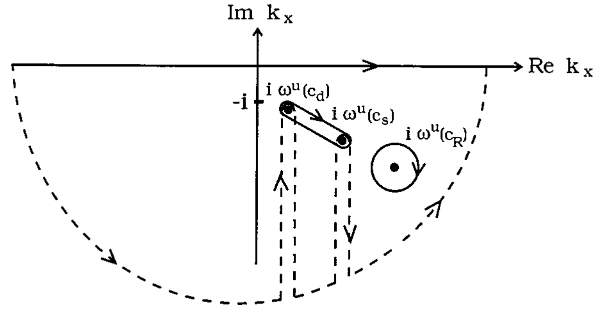

FIG. 3. The contour of integration.

knowledge of the weight function near the crack tip and on the crack surface. In this section we will expand the mode II weight function up to $r=\sqrt{X^2+y^2}$, where r is the distance from the crack tip in the comoving frame. As we only have the weight function in Fourier coordinates (with respect to k_x) we first need to relate the near crack tip expansion in real space to the corresponding terms in Fourier space. To leading order in k_x the Fourier back transforms are of the form (note $y\geqslant 0$)

$$W(X,y)=\frac{1}{2\pi}\int_{-\infty}^{\infty}dk_x e^{ik_xX}e^{-\alpha_n|k_x|y+i(sv/c_n^2\alpha_n)\mathrm{sgn}(k_x)y}\hat{W}(k_x), \tag{84}$$

which can be regarded as two Laplace transforms in y. If $\hat{W}(k_x)\rightarrow a_\beta k_x^\beta$ as $k_x\rightarrow+\infty$; then

$$W(X,y)=\frac{1}{2\pi}a_\beta\Gamma(1+\beta)2\,\mathrm{Re}\left(\frac{e^{-\alpha_n|k_x|y+i(sv/c_n^2\alpha_n)\mathrm{sgn}(k_x)y}}{(-iX+\alpha_n y)^{1+\beta}}\right), \tag{85}$$

where $\Gamma(x)$ denotes the gamma function. In our analysis it is useful to note that $\Gamma(1+x)=x\Gamma(x)$ and $\Gamma(-3/2)=\frac{4}{3}\sqrt{\pi}$. Application of Eq. (85) to the Fourier transformed weight functions in Eqs. (42) and (43) and some straightforward algebra yields the asymptotic expansion of the real space mode II weight function near the crack tip:

$$\begin{aligned}
W_{\mathrm{II},x}(X,y,k_z,s)=&\frac{-2}{1-\alpha_S^2}\frac{c_2\left(\frac{s}{v|k_z|}\right)}{c_2(0)}\frac{1}{\sqrt{2\pi}}\mathrm{Im}\left(\frac{1+i\frac{sv}{c_D^2\alpha_D}y}{\sqrt{X+i\alpha_D y}}-\frac{1+i\frac{sv}{c_S^2\alpha_S}y}{\sqrt{X+i\alpha_S y}}\right)-\frac{4}{1-\alpha_S^2}\left[\frac{c_1\left(\frac{s}{v|k_z|}\right)}{c_2(0)}|k_z|\right.\\
&\left.+\frac{c_2\left(\frac{s}{v|k_z|}\right)}{c_2(0)}\left(\frac{\omega^u(c_S)}{2}+a_0|k_z|-\omega^u(c_R)+\alpha_S^2\frac{\omega^u(c_S)+\omega^d(c_S)}{1-\alpha_S^2}\right)\right]\frac{1}{\sqrt{2\pi}}\mathrm{Im}(\sqrt{X+i\alpha_D y}\\
&-\sqrt{X+i\alpha_S y})-\frac{c_2\left(\frac{s}{v|k_z|}\right)}{c_2(0)}\frac{1}{\sqrt{2\pi}}\mathrm{Im}\left(\frac{1+i\frac{sv}{c_S^2\alpha_S}y}{\sqrt{X+i\alpha_S y}}\right)\\
&-2\left[\frac{c_1\left(\frac{s}{v|k_z|}\right)}{c_2(0)}|k_z|+\frac{c_2\left(\frac{s}{v|k_z|}\right)}{c_2(0)}\left(\frac{\omega^u(c_S)}{2}+a_0|k_z|-\omega^u(c_R)\right)\right]\frac{\mathrm{Im}\sqrt{X+i\alpha_S y}}{\sqrt{2\pi}},
\end{aligned} \tag{86}$$

$$\begin{aligned}
W_{\mathrm{II},y}(X,y,k_z,s)=&\frac{1+\alpha_S^2}{\alpha_S(1-\alpha_S^2)}\frac{c_2\left(\frac{s}{v|k_z|}\right)}{c_2(0)}\frac{1}{\sqrt{2\pi}}\mathrm{Re}\left(\frac{1+i\frac{sv}{c_S^2\alpha_S}y}{\sqrt{X+i\alpha_S y}}\right)-\frac{2\alpha_D}{1-\alpha_S^2}\frac{c_2\left(\frac{s}{v|k_z|}\right)}{c_2(0)}\frac{1}{\sqrt{2\pi}}\mathrm{Re}\left(\frac{1+i\frac{sv}{c_D^2\alpha_D}y}{\sqrt{X+i\alpha_D y}}\right)\\
&+\frac{2}{\alpha_S(1-\alpha_S^2)}\left[(1+\alpha_S^2)\frac{c_1\left(\frac{s}{v|k_z|}\right)}{c_2(0)}|k_z|+(1+\alpha_S^2)\frac{c_2\left(\frac{s}{v|k_z|}\right)}{c_2(0)}\left(\frac{\omega^u(c_S)}{2}+a_0|k_z|-\omega^u(c_R)\right)\right.\\
&\left.+\left(\alpha_S^2+\frac{(1+\alpha_S^2)(3\alpha_S^2-1)}{2(1-\alpha_S^2)}\right)\frac{c_2\left(\frac{s}{v|k_z|}\right)}{c_2(0)}(\omega^u(c_S)+\omega^d(c_S))\right]\frac{\mathrm{Re}\sqrt{X+i\alpha_S y}}{\sqrt{2\pi}}-\frac{4\alpha_D}{1-\alpha_S^2}\left[\frac{c_1\left(\frac{s}{v|k_z|}\right)}{c_2(0)}|k_z|\right.\\
&+\frac{c_2\left(\frac{s}{v|k_z|}\right)}{c_2(0)}\left(\frac{\omega^u(c_S)}{2}+a_0|k_z|-\omega^u(c_R)\right)+\left(\frac{3\alpha_S^2-1}{2(1-\alpha_S^2)}\right)\frac{c_2\left(\frac{s}{v|k_z|}\right)}{c_2(0)}(\omega^u(c_S)+\omega^d(c_S))\\
&\left.+\frac{1}{2}\frac{c_2\left(\frac{s}{v|k_z|}\right)}{c_2(0)}(\omega^u(c_S)+\omega^d(c_S)+\omega^u(c_D)+\omega^d(c_D))\right]\frac{\mathrm{Re}\sqrt{X+i\alpha_D y}}{\sqrt{2\pi}}+p_0,
\end{aligned} \tag{87}$$

$$W_{\mathrm{II},z}(X,y,k_z,s)=\frac{-4k_z}{1-\alpha_S^2}\frac{c_2\left(\frac{s}{v|k_z|}\right)}{c_2(0)}\frac{1}{\sqrt{2\pi}}\,\mathrm{Im}\left(\left(1+i\frac{sv}{c_S^2\alpha_S}y\right)\sqrt{X+i\alpha_S y}-\left(1+i\frac{sv}{c_D^2\alpha_D}y\right)\sqrt{X+i\alpha_D y}\right)$$
$$-\frac{8}{3}\frac{k_z}{1-\alpha_S^2}\left[\frac{c_1\left(\frac{s}{v|k_z|}\right)}{c_2(0)}|k_z|+\frac{c_2\left(\frac{s}{v|k_z|}\right)}{c_2(0)}\left(\frac{\omega^u(c_S)}{2}+a_0|k_z|-\omega^u(c_R)+\frac{\alpha_S^2}{1-\alpha_S^2}(\omega^u(c_S)+\omega^d(c_S))\right)\right]$$
$$\times\frac{1}{\sqrt{2\pi}}\,\mathrm{Im}((X+i\alpha_S y)^{3/2}-(X+i\alpha_D y)^{3/2})+2k_z\left(\frac{c_2\left(\frac{s}{v|k_z|}\right)}{c_2(0)}-\frac{D}{\alpha_S(1-\alpha_S^2)c_2(0)}\right)$$
$$\times\frac{1}{\sqrt{2\pi}}\,\mathrm{Im}\left(\left(1+i\frac{sv}{c_S^2\alpha_S}y\right)\sqrt{X+i\alpha_S y}\right)+\frac{4}{3}k_z\left[\frac{c_1\left(\frac{s}{v|k_z|}\right)}{c_2(0)}|k_z|+\frac{c_2\left(\frac{s}{v|k_z|}\right)}{c_2(0)}\left(\frac{\omega^u(c_S)}{2}+a_0|k_z|-\omega^u(c_R)\right)\right.$$
$$\left.+\frac{D}{2\alpha_S(1-\alpha_S^2)c_2(0)}\omega^u(c_S)\right]\frac{1}{\sqrt{2\pi}}\,\mathrm{Im}(X+i\alpha_S y)^{3/2} \tag{88}$$

as $r=\sqrt{X^2+y^2}\to 0$. The constant a_0 originates in the asymptotic expansion of $S^u(k_x)$ in Eqs. (67) or (82), i.e., $S^u(k_x)=1+ia_0(|k_z|/k_x)$, with

$$a_0=\frac{1}{|k_z|}\sum_{j=1}^{N}\Delta\eta_j\left(\omega^u\left(\frac{c_S}{\sqrt{u_2(\eta_j)}}\right)-\omega^u\left(\frac{c_S}{\sqrt{u_1(\eta_j)}}\right)\right). \tag{89}$$

The coefficients $c_1(s/v|k_z|)$ and $c_2(s/v|k_z|)$ are defined in Eqs. (40) and (41). We have also used the relationship (46) to eliminate c_0. The constant p_0 in the asymptotic expansion of $W_{\mathrm{II},y}(X,y,k_z)$ is given by [see Eq. (90), Sec. VI] $p_0=W_{\mathrm{II},y}(X=0^-,y=0,s)$.

VI. $W_{\mathrm{II},Y}$ IN REAL SPACE ON THE CRACK SURFACE

For our final evaluation of K_{II} we shall also need the full real space expression of $W_{\mathrm{II},y}$ on the crack surface. Note that the Fourier back transformation of $\hat{W}_{\mathrm{II},y}$ with respect to k_x can be turned into a contour integral in the lower complex half plane; see the dashed line in Fig. 3. In Fourier space the function $\hat{W}_{\mathrm{II},y}$ relates to Λ_2^u [also see Eq. (43)], and, hence, it has a pole and branch cuts in the lower half plane. As the simple pole at $k_x=i\omega^u(c_R)$ does not lie between the semi-infinite branch cuts we can move these branch cuts to a single finite branch cut along the line between $i\omega^u(c_D)$ and $i\omega^u(c_S)$; see Fig. 3. Then the Fourier back transform collapses to an integral along the finite branch cut between $i\omega^u(c_D)$ and $i\omega^u(c_S)$ and a circle around the pole at $k_x=i\omega^u(c_R)$ (see the solid lines in Fig. 3), yielding

$$W_{\mathrm{II},y}(X,y=0,k_z,s)=-\frac{1}{\sqrt{2\alpha_S}}\left(\frac{c_1\left(\frac{s}{v|k_z|}\right)}{c_2(0)}|k_z|-\frac{c_2\left(\frac{s}{v|k_z|}\right)}{c_2(0)}\omega^u(c_R)\right)\frac{\gamma_S^2(i\omega^u(c_R))-\omega^u(c_R)^2+k_z^2}{2(k_z^2-\omega^u(c_R)^2)\gamma_S^d(i\omega^u(c_R))S^u(i\omega^u(c_R))}e^{-\omega^u(c_R)X}$$
$$-\frac{2D}{\pi\sqrt{2\alpha_S}(1-\alpha_S^2)}\,\mathrm{sgn}\,[\mathrm{Re}(i\omega^u(c_S)-i\omega^u(c_D))](i\omega^u(c_S)-i\omega^u(c_D))e^{-\omega^u(c_D)X}$$
$$\times\int_0^1 d\tau\, e^{-\tau X(\omega^u(c_S)-\omega^u(c_D))}\left\{\left(\frac{c_1\left(\frac{s}{v|k_z|}\right)}{c_2(0)}|k_z|+ik_x\frac{c_2\left(\frac{s}{v|k_z|}\right)}{c_2(0)}\right)(ik_x+\omega^d(c_R))\right.$$
$$\left.\times\frac{(\gamma_S(k_x)^4-(k_x^2+k_z^2)^2)S^d(k_x)\gamma_S^u(k_x)\gamma_D(k_x)}{(\gamma_S(k_x)^2+k_x^2+k_z^2)^4-16\gamma_S(k_x)^2\gamma_D(k_x)^2(k_x^2+k_z^2)^2}\right\}_{\text{at } k_x=i\omega^u(c_D)+\tau(i\omega^u(c_S)-i\omega^u(c_D))} \tag{90}$$

for $X \leqslant 0$. Note also that we have replaced S^u by an expression of the form $S^u \sim r(k_x)/S^d$ [see Eq. (29)] in the integral of the above equation. This has been done for numerical reasons since by construction S^d is better approximated along the upper branch cut than S^u. For real s we need to take the limit $s+i0^+$ or $s+i0^-$ so as the prefactor $\mathrm{sign}[\mathrm{Re}(i\omega^u(c_S)-i\omega^u(c_D))]$ provides the right sign and is not exactly zero. We observe that the y component of the mode II function on the crack surface has a Taylor expansion in x of the form $W_{\mathrm{II},y}(X,y=0,s)=p_0+p_1X+\cdots$ near the crack tip (for $x \leqslant 0$). Furthermore, $W_{\mathrm{II},y}$ decays exponentially with x as $e^{-\omega^u(c_D)|x|}$. We know from Sec. V that in forward direction $(X>0)$ $W_{\mathrm{II},y}$ has an expansion in $\sqrt{X}$ of the form $W_{\mathrm{II},y}(X,y=0,s)=\cdots 1/\sqrt{X}+p_0+\cdots\sqrt{X}$ near the crack tip.

VII. CONCLUSION

It is very unlikely that a closed form exists, without quadrature or approximation, for the full time space dependent weight functions for a moving crack in three dimensions. The key difficulty is the Wiener-Hopf factorization of the Rayleigh function, and here we have contributed an approach to the quadrature required. This leads to explicit forms for approximants to the weight functions, as a function of height above the crack plane and Fourier transformed with respect to the other coordinates. The only quantity which enters our approximants nonparametrically is Poisson's ratio, but it is otherwise universal to isotropic linear elastic materials. It is likely that the same methodology would apply to anisotropic materials, at least when the fracture geometry is aligned to principal material axis, but we have not investigated this.

We applied our methods to extracting specific details of the mode II weight function in real space coordinates, in order to service our calculations of mode I crack stability in the following paper. Full real space dependence requires numerical Fourier integrals, and it is vital here that our approach give explicit functions of the Fourier variables. This spares us the full computational cost of one multiplicity of quadrature.

Other possible applications of our results include the coupling of cracks with sound, and the deflection of moving cracks by inhomogeneity. However, to carry these forward in full rests on the coupling of stress intensity to perturbation of crack geometry, which is the subject of our following paper.

ACKNOWLEDGMENT

A. A. Al-Falou was funded by EPSRC.

APPENDIX A: NOTATION AND DEFINITIONS

$E=\left[\left(\frac{\partial}{\partial t}-v\frac{\partial}{\partial X}\right)^2-\boldsymbol{\nabla}\cdot\mathbf{C}:\boldsymbol{\nabla}\right]$	Elasticity operator in comoving frame
$B=\underline{n}\cdot\mathbf{C}:\boldsymbol{\nabla}$	Boundary operator
$\underline{\sigma}[\underline{w}]=\mathbf{C}:\boldsymbol{\nabla}\underline{w}$	Stress tensor generated by the vector field $\underline{w}$
$\mathbf{C}$	Tensor of linear homogeneous, isotropic elasticity with components $C_{ijkl}=\lambda\delta_{ij}\delta_{kl}+\mu(\delta_{ik}\delta_{jl}+\delta_{il}\delta_{jk})$.
c_S	Shear wave speed
c_D	Dilatational wave speed
c_R	Rayleigh wave speed

$$\alpha_n=\sqrt{1-(v^2/c_n^2)},\quad n=S,D,R,$$

$$D=4\alpha_S\alpha_D-(1+\alpha_S^2)^2,$$

$$\omega^u\left(c_n,\frac{s}{v|k_z|}\right)=\frac{|k_z|}{\alpha_n^2}\left[\frac{s}{v|k_z|}(1-\alpha_n^2)-\sqrt{\alpha_n^2+\left(\frac{s}{v|k_z|}\right)^2(1-\alpha_n^2)}\right],\quad n=S,D,R,$$

$$\omega^d\left(c_n,\frac{s}{v|k_z|}\right)=\frac{|k_z|}{\alpha_n^2}\left[\frac{s}{v|k_z|}(1-\alpha_n^2)+\sqrt{\alpha_n^2+\left(\frac{s}{v|k_z|}\right)^2(1-\alpha_n^2)}\right],\quad n=S,D,R,$$

$$\gamma_n\left(k_x,\frac{s}{v|k_z|}\right)^2=k_x^2+k_z^2+(1-\alpha_n^2)\left(\frac{s}{v|k_z|}\left|k_z\right|-ik_x\right)^2,\quad n=S,D,R,$$

$$\gamma_n^u\left(k_x,\frac{s}{v|k_z|}\right)=\sqrt{\alpha_n i\left(i\omega^u\left(c_n,\frac{s}{v|k_z|}\right)-k_x\right)},\quad n=S,D,R,$$

$$\gamma_n^d\left(k_x,\frac{s}{v|k_z|}\right)=\sqrt{\alpha_n i\left(k_x-i\omega^d\left(c_n,\frac{s}{v|k_z|}\right)\right)},\quad n=S,D,R,$$

$$c_1\left(\frac{s}{v|k_z|}\right)=\frac{1}{2}\left[\frac{-D}{\alpha_S(1-\alpha_S^2)}\frac{\left(|k_z|-\omega^u\left(c_R,\frac{s}{v|k_z|}\right)\right)S^u\left(i|k_z|,\frac{s}{v|k_z|}\right)}{\left(|k_z|-\omega^u\left(c_S,\frac{s}{v|k_z|}\right)\right)}+\frac{\alpha_S\left(|k_z|+\omega^d\left(c_S,\frac{s}{v|k_z|}\right)\right)}{\left(|k_z|+\omega^d\left(c_R,\frac{s}{v|k_z|}\right)\right)S^d\left(-i|k_z|,\frac{s}{v\,|k_z|}\right)}\right]$$

$$c_2\left(\frac{s}{v|k_z|}\right)=\frac{1}{2}\left[\frac{D}{\alpha_S(1-\alpha_S^2)}\frac{\left(|k_z|-\omega^u\left(c_R,\frac{s}{v|k_z|}\right)\right)S^u\left(i|k_z|,\frac{s}{v|k_z|}\right)}{\left(|k_z|-\omega^u\left(c_S,\frac{s}{v|k_z|}\right)\right)}+\frac{\alpha_S\left(|k_z|+\omega^d\left(c_S,\frac{s}{v|k_z|}\right)\right)}{\left(|k_z|+\omega^d\left(c_R,\frac{s}{v|k_z|}\right)\right)S^d\left(-i|k_z|,\frac{s}{v|k_z|}\right)}\right].$$

S^u and S^d are given analytically in Eqs. (80) and (81), and numerically in Eqs. (82) and (83).

APPENDIX B: DYNAMICAL MODE II DISPLACEMENT FOR A PLANAR CRACK AND ITS FOURIER TRANSFORM

There are two different approaches to the Fourier transformed mode II displacement for a moving planar crack. Here we shall Fourier transform the real space dynamical displacements; however, alternatively, we could have determined the Fourier transformed displacements directly by the Wiener-Hopf technique as outlined in Sec. II. The calculation of the real space mode I displacement is clearly presented in Freund's book [1].

First, the mode II displacement in the comoving frame is expressed in terms of the two Lamé potentials Φ and Ψ_3, which obey the two-dimensional version of the wave equations (8) and (9). Hence both are expressible in terms of two analytic functions $G(z)$ and $F(z)$. We note that the symmetry of the type II loading yields $\Phi(x,y)=\mathrm{Im}\,F(x+i\alpha_D y)$ and $\Psi_3(x,y)=\mathrm{Re}\,F(x+i\alpha_S y)$. Then the boundary conditions on the crack face, which in terms of F and G are different from the type I case, give

$$F(z)=\frac{K_{\mathrm{II}}}{\sqrt{2\pi}\mu}\frac{8\alpha_S}{3D}z^{3/2},\qquad G(z)=\frac{K_{\mathrm{II}}}{\sqrt{2\pi}\mu}\frac{4(1+\alpha_S^2)}{3D}z^{3/2}. \tag{B1}$$

We deduce the displacements for mode II:

$$u_{\mathrm{II},x}=\frac{2K_{\mathrm{II}}}{\sqrt{2\pi}\mu D}\,\mathrm{Im}\,[2\alpha_S\sqrt{x+i\alpha_D y}-\alpha_S(1+\alpha_S^2)\sqrt{x+i\alpha_S y}], \tag{B2}$$

$$u_{\mathrm{II},y}=\frac{2K_{\mathrm{II}}}{\sqrt{2\pi}\mu D}\,\mathrm{Re}\,[2\alpha_S\alpha_D\sqrt{x+i\alpha_D y}-(1+\alpha_S^2)\sqrt{x+i\alpha_S y}]. \tag{B3}$$

In order to Fourier transform these displacement fields we first note that, for $y>0$,

$$\int_{-\infty}^{\infty}\sqrt{x+iy}\,e^{-ik_x x}dx=-\frac{1+i}{2}\frac{\sqrt{2\pi|k_x|}}{k_x^2}e^{-|k_x|y}\frac{1+\mathrm{sgn}(k_x)}{2}. \tag{B4}$$

As we can express all Fourier integrals in terms of this integral, we finally obtain the Fourier transformed mode II displacement for a planar dynamical crack ($y\geqslant 0$):

$$\hat{u}_{\mathrm{II},x}(k_x,y)=\frac{K_{\mathrm{II}}}{\sqrt{2}\mu D}[-2\alpha_S e^{-|k_x|\alpha_D y}+\alpha_S(1+\alpha_S^2)e^{-|k_x|\alpha_S y}]\frac{\sqrt{-ik_x}}{k_x^2}, \tag{B5}$$

$$\hat{u}_{\mathrm{II},y}(k_x,y)=\frac{K_{\mathrm{II}}}{\sqrt{2}\mu D}[-2\alpha_S\alpha_D e^{-|k_x|\alpha_D y}+(1+\alpha_S^2)e^{-|k_x|\alpha_S y}]\frac{\sqrt{ik_x}}{k_x^2}. \tag{B6}$$

The corresponding fields in the lower half space, $y\leqslant 0$, are given by the symmetry of the loading mode.

APPENDIX C: FOURIER TRANSFORMED 2D DYNAMICAL MODE II WEIGHT FUNCTION

We argued earlier in this paper that the weight functions can be determined on the grounds that they obey the homogeneous equations of elasticity and the boundary conditions on the crack face, and we have knowledge of their leading order divergence near the crack tip. Following this reasoning, we can deduce that the 2D weight function $\underline{W}_{2\mathrm{D,II}}$ is given by

$$\underline{W}_{2\mathrm{D,II}} \sim \frac{\partial}{\partial x} \underline{u}_{\mathrm{II}}, \tag{C1}$$

where $\underline{u}_{\mathrm{II}}$ is the mode II displacement field for a planar crack. We note that $(\partial/\partial x)\underline{u}_{\mathrm{II}}$ satisfies all the requirements on the mode II weight function. In particular, it has the right $1/\sqrt{r}$ divergence near the crack tip. The constant prefactor is determined from the condition that the weight function integral of a mode II stress field has to return the mode II stress intensity factor. In real space for $y \geqslant 0$, we then have

$$W_{2\mathrm{D,II},x} = -\frac{1}{\sqrt{2\pi}} \frac{1}{\alpha_S(1-\alpha_S^2)} \,\mathrm{Im}\left[2\alpha_S \frac{1}{\sqrt{z_d}} - \alpha_S(1+\alpha_S^2)\frac{1}{\sqrt{z_s}}\right], \tag{C2}$$

$$W_{2\mathrm{D,II},y} = -\frac{1}{\sqrt{2\pi}} \frac{1}{\alpha_S(1-\alpha_S^2)} \,\mathrm{Re}\left[2\alpha_S\alpha_D \frac{1}{\sqrt{z_d}} - (1+\alpha_S^2)\frac{1}{\sqrt{z_s}}\right], \tag{C3}$$

where $z_d = x + i\alpha_D y$ and $z_s = x + i\alpha_S y$. The original formulas for the mode II displacement field $\underline{u}_{\mathrm{II}}$ (whose derivative is taken in the above) are given in Appendix B. In Fourier space we have $(y \geqslant 0)$

$$\hat{W}_{2\mathrm{D,\,II},x}(k_x, y) = \frac{i}{\sqrt{2}\alpha_S(1-\alpha_S^2)} [2\alpha_S e^{-|k_x|\alpha_D y} - \alpha_S(1+\alpha_S^2) e^{-|k_x|\alpha_S y}] \frac{\sqrt{-ik_x}}{k_x}, \tag{C4}$$

$$\hat{W}_{2\mathrm{D,II},y}(k_x, y) = \frac{i}{\sqrt{2}\alpha_S(1-\alpha_S^2)} [2\alpha_S\alpha_D e^{-|k_x|\alpha_D y} - (1+\alpha_S^2) e^{-|k_x|\alpha_S y}] \frac{\sqrt{ik_x}}{k_x}. \tag{C5}$$

---

[1] L. B. Freund, *Dynamic Fracture Mechanics, 1990* (Cambridge University Press, Cambridge, 1990).
[2] A. A. Al-Falou and R. C. Ball (unpublished).
[3] H. F. Bueckner, Angewandte Math. Mech. **50**, 529 (1970).
[4] J. R. Rice, Int. J. Solids Struct. **8**, 751 (1972).
[5] H. F. Bueckner, Int. J. Solids Struct. **23**, 57 (1987).
[6] J. R. Willis and A. B. Movchan, J. Mech. Phys. Solids **43**, 319 (1995).
[7] A. B. Movchan and J. R. Willis, J. Mech. Phys. Solids **43**, 1369 (1995).
[8] A. A. Al-Falou and R. C. Ball, Int. J. Solids Struct. (to be published).